Original Article

NOSTRIN is involved in benign prostatic hyperplasia via inhibition of proliferation, oxidative stress, and inflammation in prostate epithelial cells

Shoubin Li[1]^, Chunhong Yu[2], Helong Xiao[1], Qingle Xu[1], Bo Gao[1], Liuxiong Guo[1], Zhanxin Sun[1], Junjiang Liu[1]

[1]Department of Urology, Hebei General Hospital, Shijiazhuang, China; [2]Health Examination Center, Hebei General Hospital, Shijiazhuang, China
Contributions: (I) Conception and design: S Li, C Yu, H Xiao; (II) Administrative support: S Li; (III) Provision of study materials or patients: S Li, Q Xu, L Guo; (IV) Collection and assembly of data: S Li, C Yu, Q Xu, B Gao, Z Sun, J Liu; (V) Data analysis and interpretation: S Li, H Xiao, B Gao, L Guo, Z Sun, J Liu; (VI) Manuscript writing: All authors; (VII) Final approval of manuscript: All authors.
Correspondence to: Shoubin Li, MD. Department of Urology, Hebei General Hospital, No. 348 Heping West Road, Shijiazhuang 050051, China. Email: hbghurology@163.com.

Background: Benign prostatic hyperplasia (BPH) is a common disease among older men characterized by non-malignant proliferation of epithelial cells and inflammation. Nitric oxide synthase traffic inducer (NOSTRIN) is a pleiotropic regulator of endothelial cell function and signaling and exerts anti-inflammatory, anti-proliferation, and modulating nuclear factor-kappa B (NF-κB) signaling effects. Its expression and function in BPH tissues and prostate epithelial cells are unknown. The study aims to investigate the expression and functions of NOSTRIN in BPH, and its possible molecular mechanism.

Methods: The BPH model was constructed in male Institute of Cancer Research (ICR) mice using 5 mg/kg/day testosterone propionate (TP) for 30 days, and the model was evaluated by detecting prostate index, prostate epithelial thickness, and prostate-specific antigen (PSA) expression. Dihydrotestosterone (DHT, 10 nM)-induced in vitro model of human prostate epithelial cells (RWPE-1) was established. We generated lentivirus-harboring human *NOSTRIN*. The mRNA expression was detected by real-time quantitative polymerase chain reaction (PCR) assay; the protein expression or localization was detected by western blot assay, immunohistochemistry, or immunofluorescence staining. Cell proliferation was assayed by 3-(4,5-dimethylthiazol-2-yl)-2,5-diphenyl tetrazolium bromide (MTT) and 5-ethynyl-2'-deoxyuridine (EdU) staining. Reactive oxygen species (ROS) production was observed by dihydroethidium staining. Nitric oxide (NO) and malondialdehyde (MDA) levels and superoxide dismutase (SOD) activity were detected using commercial kits. Enzyme-linked immunosorbent assay (ELISA) was used to determine levels of interleukin 1 beta (IL1B), interleukin 6 (IL6), interferon gamma (IFNG), and tumor necrosis factor (TNF).

Results: NOSTRIN expression was significantly inhibited in the TP-induced ICR mouse BPH model and DHT-induced model of RWPE-1 proliferation. Protein expression of the BPH-related and proliferation markers PSA and proliferating cell nuclear antigen (PCNA) was suppressed in NOSTRIN-overexpressing RWPE-1 cells exposed to DHT. NOSTRIN overexpression notably inhibited the RWPE-1 cell proliferation *in vitro*, as evidenced by MTT and EdU staining. NOSTRIN overexpression significantly decreased the expression of cell cycle-related proteins cyclin dependent kinase 4 (CDK4) and cyclin D1 (CCND1) *in vitro*. The production of ROS, NO, and lipid peroxidation products MDA was inhibited by NOSTRIN overexpression *in vitro*, while the SOD activity was increased. NOSTRIN overexpression reduced the mRNA expression of inflammatory mediator nitric oxide synthase 2 (NOS2) and inhibited the mRNA expression and secretion of pro-inflammatory cytokines IL1B, IL6, IFNG, and TNF *in vitro*. The mechanistic

^ ORCID: 0000-0002-6873-0523.

studies revealed an increased phosphorylation of NF-κB p65 *in vivo* and *in vitro*. Remarkably, NOSTRIN overexpression notably inhibited the protein expression of phospho-NF-κB p65 *in vitro*.

Conclusions: NOSTRIN is involved in BPH by inhibiting proliferation, oxidative stress, and inflammation in prostate epithelial cells. These functions may act through the inhibition of NF-κB signaling.

Keywords: Nitric oxide synthase traffic inducer (NOSTRIN); benign prostatic hyperplasia (BPH); human prostate epithelial cells (RWPE-1)

Submitted Apr 29, 2024. Accepted for publication Aug 19, 2024. Published online Sep 24, 2024.
doi: 10.21037/tau-24-209
View this article at: https://dx.doi.org/10.21037/tau-24-209

Introduction

Benign prostatic hyperplasia (BPH) is the most common urological disease in older men, with a prevalence of more than 80% among men aged 70 years or older (1). It is characterized by an excessive proliferation of prostatic epithelial and stromal cells, leading to prostate enlargement and lower urinary tract symptoms (2,3). Inflammation and oxidative stress are major contributing factors that participate in the development of BPH (4). Almost all patients with BPH showed increased immune cell infiltration, including macrophages, and accumulation of inflammatory mediators and growth factors in the tissue environment (5). In a cohort of 282 patients, 81% had T-lymphocyte markers (CD3), 52% had B-lymphocyte markers (CD20), and 82% had macrophage markers (CD163), considering the cells infiltrating BPH tissues (6). Tissue damage following inflammation and the chronic process of repetitive wound healing and tissue remodeling promote epithelial and stromal cell proliferation and facilitate BPH progression (7).

Additionally, it has commonly been assumed that testosterone-associated increase of 5α-reductase type II (5AR2) and androgen receptor (AR) exerts an effect on the pathogenesis of BPH. The 5AR2 converts testosterone to dihydrotestosterone (DHT) in the prostate. Decreased testosterone due to aging increases the expression of 5AR2 and AR to maintain DHT levels in the prostate, which leads to an imbalance in the endocrine system and prostate hyperplasia. The DHT-AR complex promotes the production of prostate-specific antigen (PSA), which contributes to BPH development (8). The many side effects associated with currently available BPH medications, including Steroid 5α-reductase inhibitors, have led to increased interest in looking for novel therapeutic targets (9).

Nitric oxide synthase traffic inducer (NOSTRIN) is originally identified as a regulator of subcellular localization and activity of endothelial nitric oxide synthase (eNOS) (10). It is commonly recognized as an endothelial cell protein with eNOS-dependent and eNOS-independent functions (11). Previous studies have shown that NOSTRIN is involved in regulating various pathological processes, including cardiovascular function, glomerular barrier function, and cancer (12-14). Chakraborty *et al.* found that ectopic NOSTRIN overexpression inhibited endothelial cell proliferation (15). Additionally, NOSTRIN has been shown to participate in inhibiting cell cycle progression (16). It is known that NOSTRIN reduces the production of NO (10), and inhibiting NO production and oxidative stress alleviates BPH (17,18). It has been reported that NOSTRIN has

Highlight box

Key findings

- Nitric oxide synthase traffic inducer (NOSTRIN) is involved in benign prostatic hyperplasia (BPH) progression.

What is known and what is new?

- Inflammation and oxidative stress are major contributing factors that participate in the development of BPH. NOSTRIN plays an important role in regulating oxidative stress and inflammation in endothelial cells.
- Increased expression of NOSTRIN inhibits proliferation, oxidative stress, and inflammation in prostate epithelial cells.

What is the implication, and what should change now?

- Our findings suggest that NOSTRIN is a potential therapeutic target for ameliorating BPH. One limitation is that we investigated the anti-inflammatory effects of NOSTRIN only in human prostate epithelial cells (RWPE-1) without correlation with immune cells such as macrophages and stromal cells. Further study is needed to explore the relationship between prostate epithelial cells and these cell types.

potent anti-inflammatory properties in endothelial cells (15). Overexpression of NOSTRIN reduced the expression of pro-inflammatory factors interleukin 6 (*Il6*), C-C motif chemokine ligand 2 (*Ccl2*), and C-C motif chemokine ligand 5 (*Ccl5*) and inhibited the activation of the nuclear factor-kappa B (NF-κB) pathway in endothelial cells (15). NF-κB is a key transcription factor involved in many biological processes including cell proliferation, oxidative stress, and inflammation (19,20). Though little is known about its role in BPH, given its known functions, we hypothesized that NOSTRIN might be involved in regulating the progression of BPH.

In this study, we investigated the NOSTRIN expression in prostate tissues in an online database and mouse BPH model. The DHT-induced model of human prostate epithelial cell (RWPE-1) proliferation was used to explore the effects of NOSTRIN in BPH. The effects of NOSTRIN on cell proliferation, inflammation, and oxidative stress and the molecular mechanisms by which NOSTRIN regulated BPH were investigated. We present this article in accordance with the ARRIVE reporting checklist (available at https://tau.amegroups.com/article/view/10.21037/tau-24-209/rc).

Methods

Animal study

A protocol was prepared before the study without registration. Experiments were performed under a project license (No. 202372) granted by the Ethics Committee of Hebei General Hospital, in compliance with institutional guidelines for the care and use of animals. Six-week-old male Institute of Cancer Research (ICR) mice were purchased from Huachuang Sino (China) and housed in a 21–23 ℃, 45–55% humidity environment with a 12-h day/night cycle. Mice had free access to food and water. Mice adapted to the new environment for 7 days prior to the experiments. Twenty-six ICR mice were randomized into two groups: the control group (12 mice) and the BPH group (14 mice). The sample size was determined based on the results of preliminary experiments and power analysis. The prostates of 6 mice were removed for histological examination and the remaining 6 mice prostates were used for molecular experiments for each group. Random numbers were generated using the standard = RAND() function in Microsoft Excel. An individual mouse was considered the experimental unit in all statistical analyses. Testosterone propionate (TP, 5 mg/kg/day, Macklin, China) diluted with soybean oil was injected subcutaneously for 30 days to produce prostatic hyperplasia (21). In parallel, the control mice received a soybean oil injection. Next, the mice were weighed, anesthesia with isoflurane, and killed by cervical dislocation. The prostate was removed and weighed. The dorsolateral prostate lobe of mice was removed for histological examination and the whole prostates were used for testing the mRNA and protein expression. Prostate index (‰) = 1000 × prostate weight (g)/body weight (g). Mice were monitored twice daily for food and water intake, general assessment of animal activity, panting, and fur condition. Mice reaching the humane endpoint of weight loss greater than 20% were euthanized. For each animal, three different investigators were involved as follows: TP or vehicle were arranged and labeled by a first researcher according to the randomization plan. He was the only person aware of the group allocation. A second investigator was responsible for performing the injections, whereas a third investigator performed the assessment. The testing order was random. The success of the BPH model was determined by examining the differences in prostate index, prostate epithelial thickness, and PSA expression with control mice. Two mice that failed to develop BPH were excluded.

Prostate histopathological analysis

The prostate tissue from mice was fixed in 4% paraformaldehyde and embedded in paraffin following conventional methods. Then, tissues were cut into 5 μm slices, deparaffinized and hydrated. For Hematoxylin-eosin (HE) staining, slices were stained with hematoxylin (Solarbio, China) for 5 min and eosin (Sangon, China) for 3 min at room temperature, respectively. For immunohistochemistry (IHC), antigen retrieval was performed by boiling slices in an antigen retrieval solution of 0.1 M citric acid and 0.1 M sodium citrate. Tissue sections were incubated with 3% hydrogen peroxide and blocked in 1% bovine serum albumin (BSA). Subsequently, anti-PSA (Cat# 10679-1-AP, RRID: AB_2134244, Proteintech, China) anti-NOSTRIN (Cat# 20116-1-AP, RRID: RRID: AB_10666167, Proteintech, China) and anti-CD68 (Cat# Ab955, RRID: AB_307338, Abcam, UK) were dripped on the tissues for incubation in a moist chamber at 4 ℃ overnight. Anti-rabbit horseradish peroxidase (HRP) secondary antibody (Cat# SE134, RRID: AB_2797593, Solarbio, China) and anti-mouse HRP secondary antibody

(Cat# SE131, RRID: AB_2797595, Solarbio, China) were used to incubate the sections for 45 min at room temperature. The final antibody concentrations of primary antibodies were 3.5 μg/mL for PSA antibody, 2 μg/mL for NOSTRIN antibody, and 0.5 μg/mL for CD68 antibody. The final antibody concentration of secondary antibody was 20 μg/mL. Next, the slices were stained using 3,3'-diaminobenzidine (DAB, Sangon, China) for 10 min at 37 ℃ and counterstained with hematoxylin (Solarbio, China) for 3 min. Finally, slices were dehydrated, mounted in neutral gum, and placed under a microscope (Olympus, Japan) to take photos and observe staining results.

Cell culture and treatment

Human normal prostate epithelial cells (RWPE-1, Cat# iCell-h286, RRID: CVCL_3791) were purchased from iCell Bioscience (China). Cells were grown in specialized media (Cat# iCell-h286-001b, iCell Bioscience, China) containing Pen/Strep. NOSTRIN overexpression (OE) plasmid pCMV3-NOSTRIN (Cat# HG14269-UT) was purchased from SinoBiological (China). Lentiviral particles were produced by the transfection of HEK293T cells with pCMV3-NOSTRIN plasmid, lentiviral packaging plasmid, and envelope plasmids. When the RWPE-1 cells reached 90% confluence, they were trypsinized and seeded into 6 well plates (for total protein and total RNA extraction) or 12 well plates [for dihydroethidium (DHE) staining]. After cell adherence, the medium was replaced by the virus-containing medium, and cells were incubated for another 48 h. RWPE-1 cells were then stimulated with 10 nM DHT for 24 h to mimic the BPH model induced by androgen (22). After 24 h of DHT exposure, cells were collected for total protein and total RNA extraction or were ready for DHE staining. Cells were cultured in a humidified incubator containing 5% CO_2 at 37 ℃.

Cell proliferation assay

3-(4,5-dimethylthiazol-2-yl)-2,5-diphenyl tetrazolium bromide (MTT) cell proliferation and cytotoxicity detection kit was obtained from KeyGEN BioTECH (China), and DHT was purchased from Abmole Bioscience Inc. (USA). RWPE-1 cells were seeded into 96 well plates at a concentration of 5×10^3 cells per well. After the cells adhered to the wall, they were exposed to DHT or both DHT and either Vector-OE or NOSTRIN-OE. At the end of treatment, 50 μL MTT solution was added to each well, and cells were incubated for an additional 4 h. After the incubation period, the supernatant was discarded carefully, and 150 μL of dimethyl sulfoxide (DMSO, KeyGEN BioTECH, China) was added to each well to dissolve the formazan crystals. Finally, a microplate reader (Biotek, USA) was used to measure the optical density (OD) value at 490 nm. The 5-ethynyl-2'-deoxyuridine (EdU) assay was performed according to the instructions of the EdU Cell Proliferation Test Kit (KeyGEN BioTECH, China). Briefly, cells were incubated with a final concentration of 10 μM EdU for 4 h in a cell culture incubator at 37 ℃, followed by incubation with the click reaction solution for 30 min at room temperature in the dark. Next, cells were washed and resuspended in the phosphate-buffered solution for further analysis via flow cytometry.

Real-time quantitative polymerase chain reaction (RT-qPCR) assay

TRIpure reagent (BioTeke, China) was used to isolate total RNA from the mouse prostate tissues and RWPE-1 cells. The RNA sample concentrations were evaluated using a Nano 2000 UV spectrophotometer (Thermo, USA) and then samples were reverse transcribed into cDNA using an All-in-One First-Strand SuperMix (Magen, China). Next, we performed RT-qPCR using Taq PCR MasterMix (Solarbio, China) and SYBR Green (Solarbio, China). Primers were synthesized by General Biol (China), and the primers used are as follows: Mus *Nostrin* F 5'-TCTCCTGGCTGACTATTT; R 5'-CCATGTCTTTCTGGCTC. Mus interferon gamma (*Ifng*) F 5'-AGTGGCATAGATGTGGAA; R 5'-CTCAAACTTGGCAATACTC. Mus nitric oxide synthase 2 (*Nos2*) F 5'-CACCACCCTCCTCGTTC; R 5'-CAATCCACAACTCGCTCC. Mus interleukin 1 beta (*Il1b*) F 5'-TTCCCATTAGACAACTGC; R 5'-GATTCTTTCCTTTGAGGC. Mus *Il6* F 5'-TAACAGATAAGCTGGAGTC; R 5'-TAGGTTTGCCGAGTAGA. Mus tumor necrosis factor (*Tnf*) F 5'-TTCTCATTCCTGCTTGTGG; R 5'-CACTTGGTGGTTTGCTACG. Homo *NOSTRIN* F 5'-CCTGGAACGAATGCTTA; R 5'-GGCTGGGTTGAGGTCTT. Homo *IFNG* F 5'-ATTCAGATGTAGCGGATAA; R 5'-ATTGCTTTGCGTTGGAC. Homo *NOS2* F 5'-AGCGGTAACAAAGGAGATAG; R 5'-GGGAACACGGTGATGG. Homo *IL1B* F 5'-TATTACAGTGGCAATGAGG;

R 5'-ATGAAGGGAAAGAAGGTG. Homo *IL6* F 5'-GTCCAGTTGCCTTCTCCC; R 5'-GCCTCTTTGCTGCTTTCA. Homo *TNF* F 5'-CGAGTGACAAGCCTGTAGCC; R 5'-TGAAGAGGACCTGGGAGTAGAT. All samples were analyzed using the $2^{-\Delta\Delta CT}$ method. Data were normalized to the expression of β-actin.

Western blot (WB) assay

Total protein was extracted from mouse prostate tissues and RWPE-1 cells using RIPA lysis buffer (Proteintech, China) containing protease inhibitors (Proteintech, China). Protein quantification was conducted using the bicinchoninic acid (BCA) protein concentration detection kit (Proteintech, China). Proteins were separated by 11% SDS-polyacrylamide gel electrophoresis (SDS-PAGE) and were transferred to the polyvinylidene fluoride (PVDF) membrane (Thermo, USA). After blocking with Tris-buffered saline/Tween-20 (TBST) containing 5% skimmed milk powder for 2 h, the membranes were incubated with primary antibodies at 4 ℃ overnight and secondary antibodies for 40 min at 37 ℃, respectively. All antibodies were diluted in antibody diluent (Proteintech, China). Antibodies and the final antibody concentrations are as follows. Anti-NOSTRIN antibody, Cat# sc-365031 (RRID: AB_10852498, Santa, USA), 0.667 μg/mL; anti-PSA antibody, Cat# AF0246 (RRID: AB_2833421, Affinity, China), 2 μg/mL; anti-Proliferating Cell Nuclear Antigen (PCNA) antibody Cat# AF0239 (RRID: AB_2833414, Affinity, China), 2 μg/mL; anti-phospho-NF-κB p65 antibody Cat# AF2006 (RRID: AB_2834435, Affinity, China), 1 μg/mL; anti-NF-κB p65 antibody, Cat# AF5006 (RRID: AB_2834847, Affinity, China), 1 μg/mL; anti-cyclin D1 (CCND1) antibody, Cat# DF6386 (RRID: AB_2838349, Affinity, China), 2 μg/mL; anti-cyclin dependent kinase 4 (CDK4) antibody, Cat# AF4034 (RRID: AB_2835341, Affinity, China), 2 μg/mL; anti-β-actin antibody, Cat# 66009-1-Ig (RRID: AB_2687938, Proteintech, China), 0.05 μg/mL; goat anti-mouse IgG secondary antibody, Cat# SA00001-1 (RRID: AB_2722565, Proteintech, China), 0.02 μg/mL; goat anti-rabbit IgG secondary antibody, Cat# SA00001-2 (RRID: AB_2722564, Proteintech, China), 0.02 μg/mL. The protein bands were detected using an ultrasensitive ECL chemiluminescence detection kit (Proteintech, China) and exposed to X-ray film. Next, the film was scanned, and Gel-Pro Analyzer software was used to calculate the optical density.

Dihydroethidium staining

The mouse prostate tissue fixed in 4% paraformaldehyde was sucrose infiltrated and embedded in the optimal cutting temperature (OCT) embedding agent before freezing and cutting on cryostat microtome (Leica, Germany). Slices (10 μm thick) were incubated with DHE solution (Beyotime, China) for 30 min at 37 ℃ in the dark. Subsequently, the cover slides were placed on tissue with an anti-fluorescence quencher. For cells, a final concentration of 5 μM DHE was added to each well and incubated for 30 min in the dark at the end of the experiment. Reactive oxygen species (ROS)-derived fluorescence (red) was analyzed under a microscope.

Immunofluorescence (IF) staining

RWPE-1 cells were seeded on cover slides in well plates. After treating cells with DHT or both DHT and either Vector-OE or NOSTRIN-OE as described above, cells were fixed in 4% paraformaldehyde and incubated with 0.1% tritonX-100 (Beyotime, China) for 30 min at room temperature. Then, cells were blocked in the blocking solution (1% BSA) for 15 min and probed with phospho-NF-κB p65 antibody (0.125 μg/mL, Cat# AP0124, RRID: AB_2771510, Abclonal, China). After incubation with the primary antibody overnight at 4 ℃, cells were incubated for 60 min with Cy3-conjugated secondary antibody (Cy3-Goat Anti-Rabbit IgG, 1 μg/mL, Cat# SA00009-2, RRID: AB_2890957, Proteintech, China). For nuclear staining, 4',6-diamidino-2-phenylindole (DAPI, Aladdin, China) was applied to cells. Following washing, the slides were mounted by an anti-fluorescence quencher (Solarbio, China) and processed for fluorescence microscopy. Images were taken under a microscope.

Enzyme-linked immunosorbent assay (ELISA) detection

Commercially available ELISA kits (Liankebio, China) were utilized for the detection of human IL1B (EK101B), IL6 (EK106), TNF (EK182), and IFNG (EK180). At the end of the cell experiment, cell supernatant was collected and assays were performed following the manufacturer's instructions.

Detection of superoxide dismutase (SOD) activity, and contents of malondialdehyde (MDA) and nitric oxide (NO)

Nanjing Jiancheng Bioengineering Institute (China)

provided SOD, MDA, and NO assay kits. Cells were harvested by centrifugation and lysed by sonication. The SOD activity and the levels of MDA and NO using the hydroxylamine method, the thiobarbituric acid (TBA) method, and the nitrate reductase method based on the manufacturer's protocol, respectively.

Statistical analysis

Data were graphed as mean ± standard deviation (SD) with 3 (for cell study)-6 (for animal study) biological replicates and analyzed using GraphPad Prism 9.5 software (RRID: SCR_002798). The statistical analysis was performed using the one-way analysis of variance (one-way ANOVA) or *t*-test. Appropriate non-parametric tests were used if the data did not meet the assumptions of the intended parametric test (normality, heterogeneity of variance tests). A P value <0.05 is considered statistically significant and marked in the figures. The non-significant differences are unmarked.

Results

NOSTRIN expression in BPH tissues and construction of the animal BPH model

We analyzed the expression of NOSTRIN in the human BPH dataset GSE119195 from the public Gene Expression Omnibus (GEO) database. As shown in *Figure 1A*, NOSTRIN was significantly lower expressed in human BPH tissues than in normal prostate tissues. To verify the NOSTRIN expression in tissues with BPH, we constructed a TP-induced BPH mouse model. The animal BPH model construction process was summarized in the study schematic shown in *Figure 1B*. In the study, mice treated with TP exhibited a significant increase in the prostate index (*Figure 1C*). In HE staining (*Figure 1D*), it can be observed that epithelial thickness was increased and stromal cellular proliferation in the prostate after TP administration. Elevated PSA levels suggest an increased risk of prostate size enlargement and prostatic hyperplasia (8). Immunohistochemical and quantitative results showed that PSA expression was significantly increased in the prostate tissues of mice injected with TP (*Figure 1E*,*1F*). These results indicated that the TP-induced BPH model in mice was successfully established. Remarkably, the mRNA and protein expression of NOSTRIN was diminished in the hyperplastic prostate of mice (*Figure 1G*). NOSTRIN had the same expression trend in immunohistochemical staining (*Figure 1H*).

Oxidative stress and inflammation in the prostate of BPH mice

The DHE staining was performed to detect oxidative stress in the prostate of mice. Intense red fluorescence was observed in the prostate tissues of mice with BPH (*Figure 2A*). Moreover, the relative mRNA expression levels of inflammatory mediators *Nos2*, *Il1b*, *Il6*, *Tnf*, and *Ifng* were significantly increased in the hyperplastic prostate of mice (*Figure 2B*). The phosphorylated NF-κB p65 levels were induced in the BPH tissues of mice (*Figure 2C*), implying that the NF-κB pathway was activated. These results suggested that NF-κB signaling was activated with increased oxidative stress and inflammation. As presented in the IHC images (*Figure 2D*), CD68-positive ($CD68^+$) cells (including macrophages and monocytes) accumulated in the prostate tissues of mice with BPH.

NOSTRIN overexpression inhibits cell proliferation by downregulating cell cycle-related proteins in DHT-induced RWPE-1 cells

To investigate the effects of NOSTRIN on RWPE-1 cells, we established NOSTRIN overexpressing cells using lentivirus and exposed the cells to DHT to mimic BPH conditions *in vitro*. The expression of NOSTRIN in cells was verified by RT-qPCR and WB (*Figure 3A*). As illustrated in *Figure 3B*, NOSTRIN overexpression significantly inhibited the protein expression of PSA in cells exposed to DHT, indicating that NOSTRIN attenuated BPH progression *in vitro*. PCNA expression is consistent with DNA synthesis during cell proliferation and can be used to evaluate cell proliferation. The PCNA protein expression was significantly decreased in DHT-treated cells overexpressing NOSTRIN (*Figure 3B*). MTT results showed that NOSTRIN overexpression significantly reduced OD values in DHT-induced RWPE-1 cells (*Figure 3C*). These results were further confirmed by EdU staining (*Figure 3D*), suggesting that the overexpression of NOSTRIN inhibited the proliferation of RWPE-1 cells exposed to DHT. The interaction of cell cycle-related proteins CDK4 and CCND1 promotes G1-S cell cycle transition and cell proliferation (23). In NOSTRIN-overexpressed RWPE-1 cells, CDK4 and CCND1 protein expression were dramatically inhibited (*Figure 3E*). These

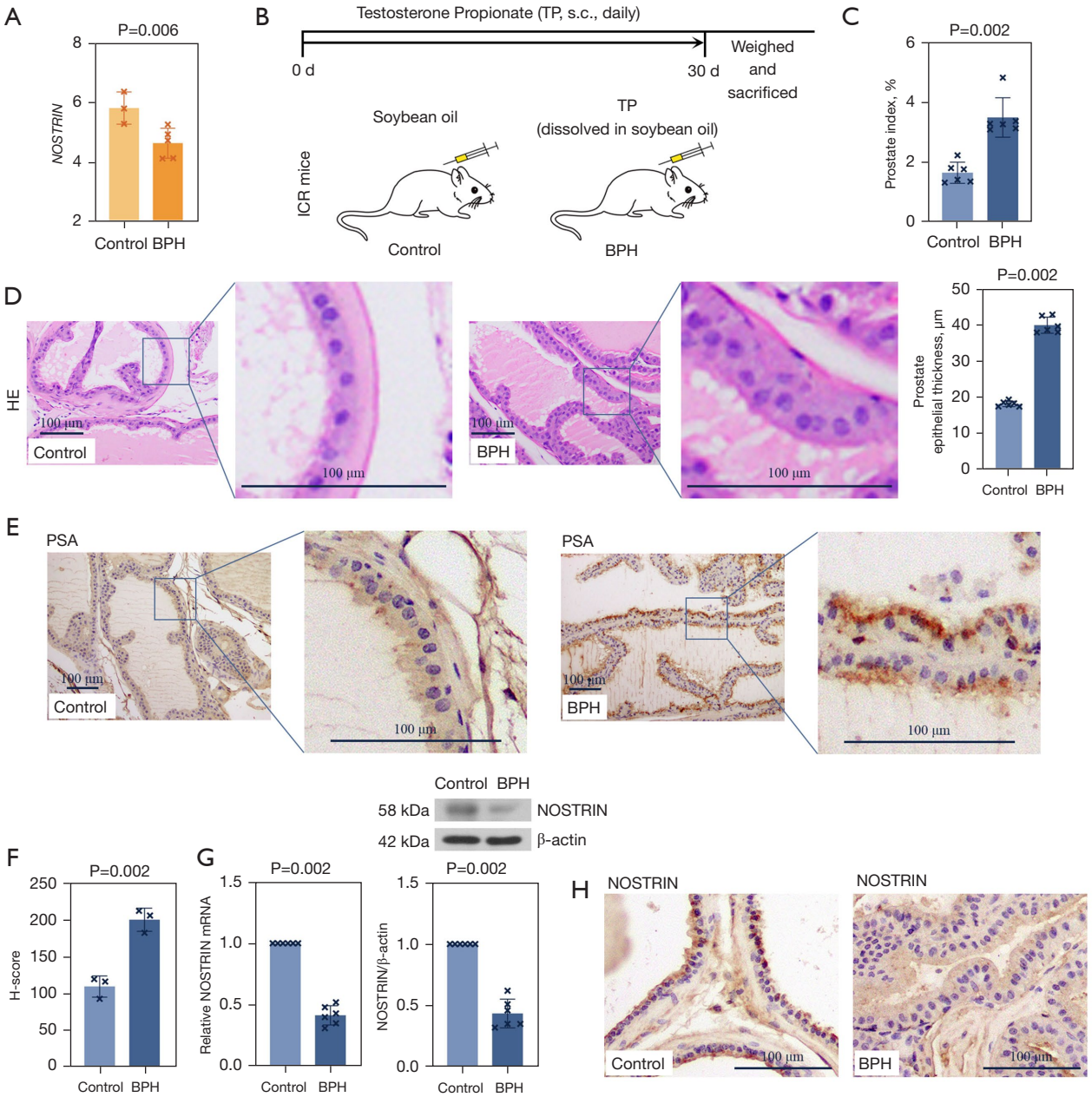

Figure 1 NOSTRIN expression in BPH tissues and construction of the animal BPH model. (A) The *NOSTRIN* expression in human prostatic tissue from the GEO database (accession number: GSE119195). (B) Experimental flow chart of TP-induced animal model. (C) Prostate index. (D) Histopathological examination of prostate in mice for observation of epithelial thickness by HE staining (200×). Determination of prostate epithelial thickness. (E) Immunohistochemical images (200×) of PSA. (F) Analysis of the PSA staining by a semi-quantitative histological score (H-score). (G) NOSTRIN mRNA and protein expression in the prostate of mice was detected using real-time PCR and Western blot, respectively. Data are shown as mean ± standard deviation. (H) Immunohistochemical staining of NOSTRIN in mice prostate (200×). The P value and scale bar are marked in the figure. NOSTRIN, Nitric oxide synthase traffic inducer; ICR mice, Institute of Cancer Research mice; BPH, benign prostatic hyperplasia; GEO, Gene Expression Omnibus; TP, testosterone propionate; HE, hematoxylin-eosin; PSA, prostate-specific antigen; PCR, polymerase chain reaction.

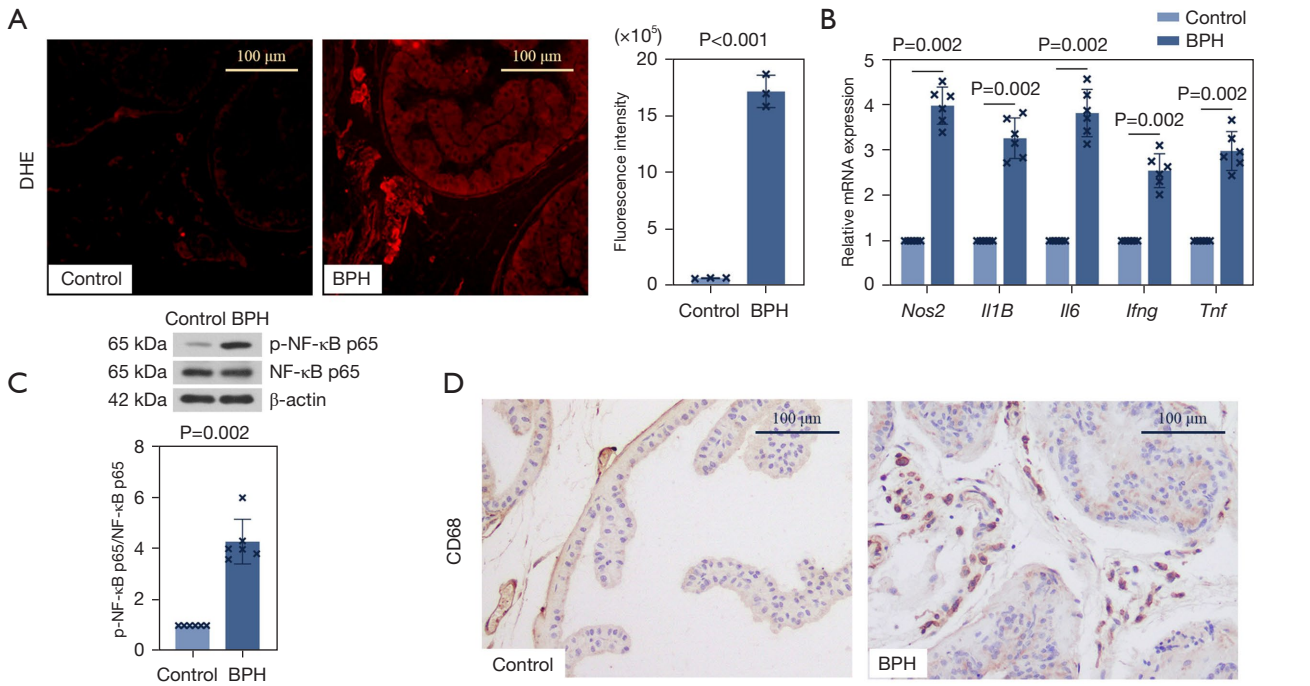

Figure 2 Oxidative stress and inflammation in the prostate of BPH mice. (A) ROS content was assayed by DHE staining (200×). Quantification of the fluorescence intensity of DHE staining. (B) Nitric oxide synthase 2 (*Nos2*), interleukin 1 beta (*Il1b*), interleukin 6 (*Il6*), interferon gamma (*Ifng*), and tumor necrosis factor (*Tnf*) mRNA expression levels determined by real-time PCR analysis. (C) NF-κB p65 and phospho-NF-κB p65 (p-NF-κB p65) expression in mice prostate detected by Western blot assay. (D) Immunohistochemistry staining (200×) of CD68 in mouse prostate tissues. Data are shown as mean ± standard deviation. The P value and scale bar are marked in the figure. BPH, benign prostatic hyperplasia; ROS, reactive oxygen species; DHE, dihydroethidium; NF-κB, nuclear factor-kappa B; PCR, polymerase chain reaction.

results showed that NOSTRIN inhibited RWPE-1 cell proliferation *in vitro* by suppressing cell cycle progression.

NOSTRIN overexpression reduces oxidative stress and inflammation and inhibits NF-κB signaling in DHT-induced RWPE-1 cells

In DHE staining and the quantitative results (*Figure 4A*), it can be seen that the overexpression of NOSTRIN markedly decreased ROS levels in cells stimulated by DHT. We observed elevated SOD activities (*Figure 4B*) and reduced MDA and NO levels (*Figure 4C*) in NOSTRIN overexpressed cells exposed to DHT, implying that NOSTRIN inhibited oxidative stress *in vitro*. NOSTRIN overexpression significantly inhibited the mRNA expression levels of inflammatory mediators *NOS2*, *IL1B*, *IL6*, *IFNG*, and *TNF* when RWPE-1 cells were treated with DHT (*Figure 4D*). Furthermore, in the supernatant of DHT-induced RWPE-1 cells, the content of secreted IL1B, IL6, TNF, and IFNG showed a trend similar to that of the mRNA transcript levels (*Figure 4E*). WB results showed that the NF-κB p65 phosphorylation level was significantly declined in NOSTRIN-overexpressing RWPE-1 cells upon DHT stimulation (*Figure 4F*). IF staining further confirmed this result. As illustrated in *Figure 4G*, nuclear phospho-NF-κB p65 levels were markedly increased in DHT-treated RWEP-1 cells; however, this effect was significantly attenuated following the overexpression of NOSTRIN. These findings showed that NOSTRIN overexpression reduced oxidative stress and inflammation *in vitro*, while NF-κB activation was inhibited.

Discussion

In this study, we investigated the NOSTRIN expression in mouse BPH tissues, its roles in prostate epithelial cells, and its possible mechanism of action. NOSTRIN is found to inhibit NO production in endothelial cells by regulating the

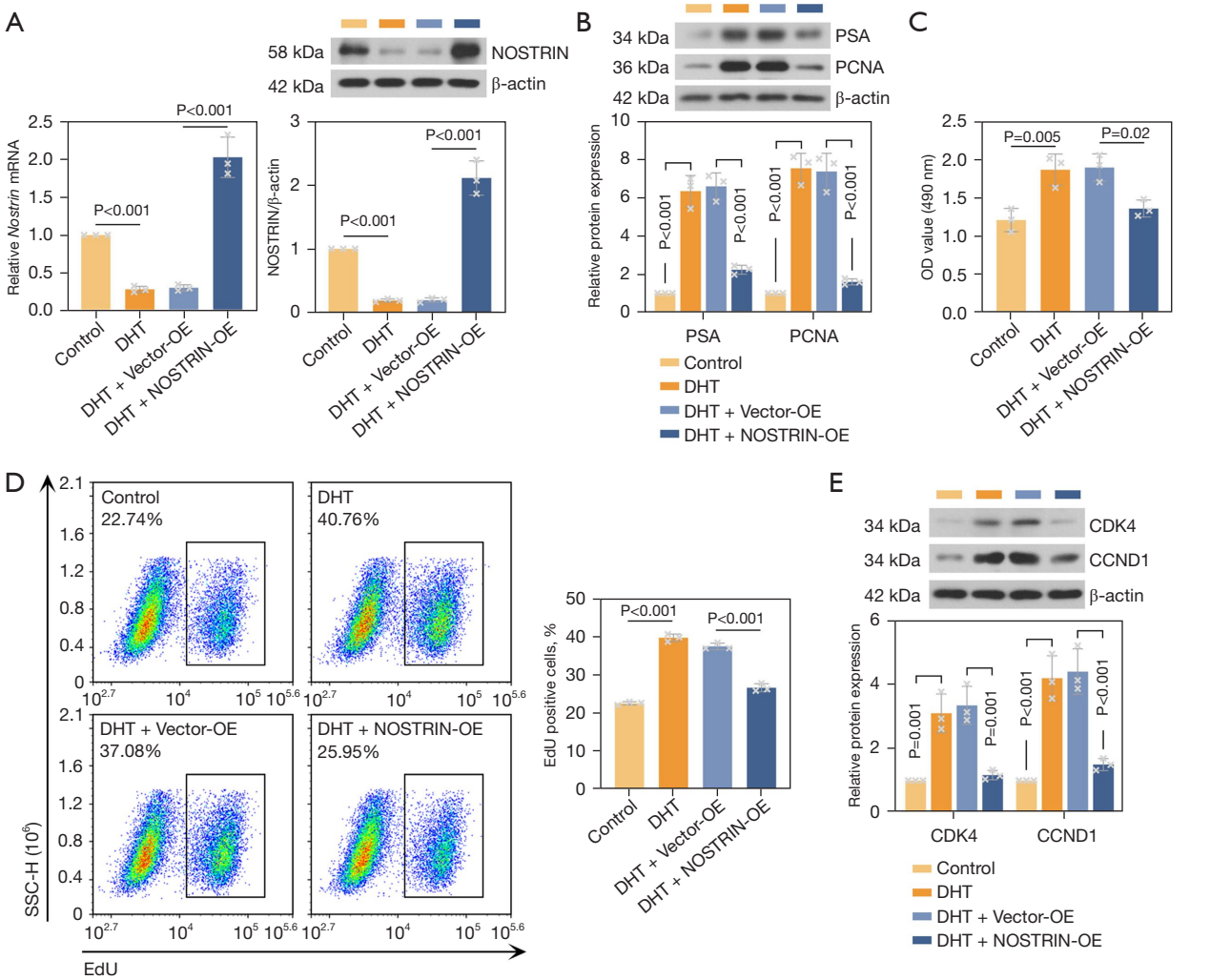

Figure 3 NOSTRIN overexpression inhibits cell proliferation by downregulating cell cycle-related proteins in dihydrotestosterone-induced RWPE-1 cells. (A) Overexpression of NOSTRIN was verified by real-time PCR and Western blot analysis. (B) Western blot analysis of PSA and PCNA in RWPE-1 cells. (C) MTT assay was conducted to determine the RWPE-1 cell viability. (D) The proliferation of RWPE-1 cells was detected using EdU staining on flow cytometry. Quantitative analysis of EdU-positive cells. (E) The protein expression levels of CDK4 and CCND1 were detected by Western blot. Data are shown as mean ± standard deviation. The P value is marked in the figure. DHT, dihydrotestosterone; NOSTRIN, nitric oxide synthase traffic inducer; OE, overexpression; PSA, prostate-specific antigen; PCNA, proliferating cell nuclear antigen; MTT, 3-(4,5-dimethylthiazol-2-yl)-2,5-diphenyl tetrazolium bromide; EdU, 5-ethynyl-2'-deoxyuridine; CDK4, cyclin dependent kinase 4; CCND1, cyclin D1; PCR, polymerase chain reaction; OD, optical density.

intracellular distribution of eNOS (24), playing important roles in cardiovascular diseases, cancers, and other diseases (12-14). However, its expression and function in the prostate and epithelial cells are poorly understood. We searched public databases for BPH-related expression data and found that NOSTRIN expression was significantly inhibited in human BPH tissues. Considering its anti-inflammatory and antiproliferative properties in endothelial cells, we hypothesized that the involvement of NOSTRIN can ameliorate BPH with similar effects.

In this study, the mRNA and protein expression of NOSTRIN in mouse prostate hyperplasia tissues were consistent with the results analyzed from public databases. The NOSTRIN expression was also inhibited in DHT-induced human prostatic epithelial cells. PSA is a glycoprotein produced exclusively by the prostatic

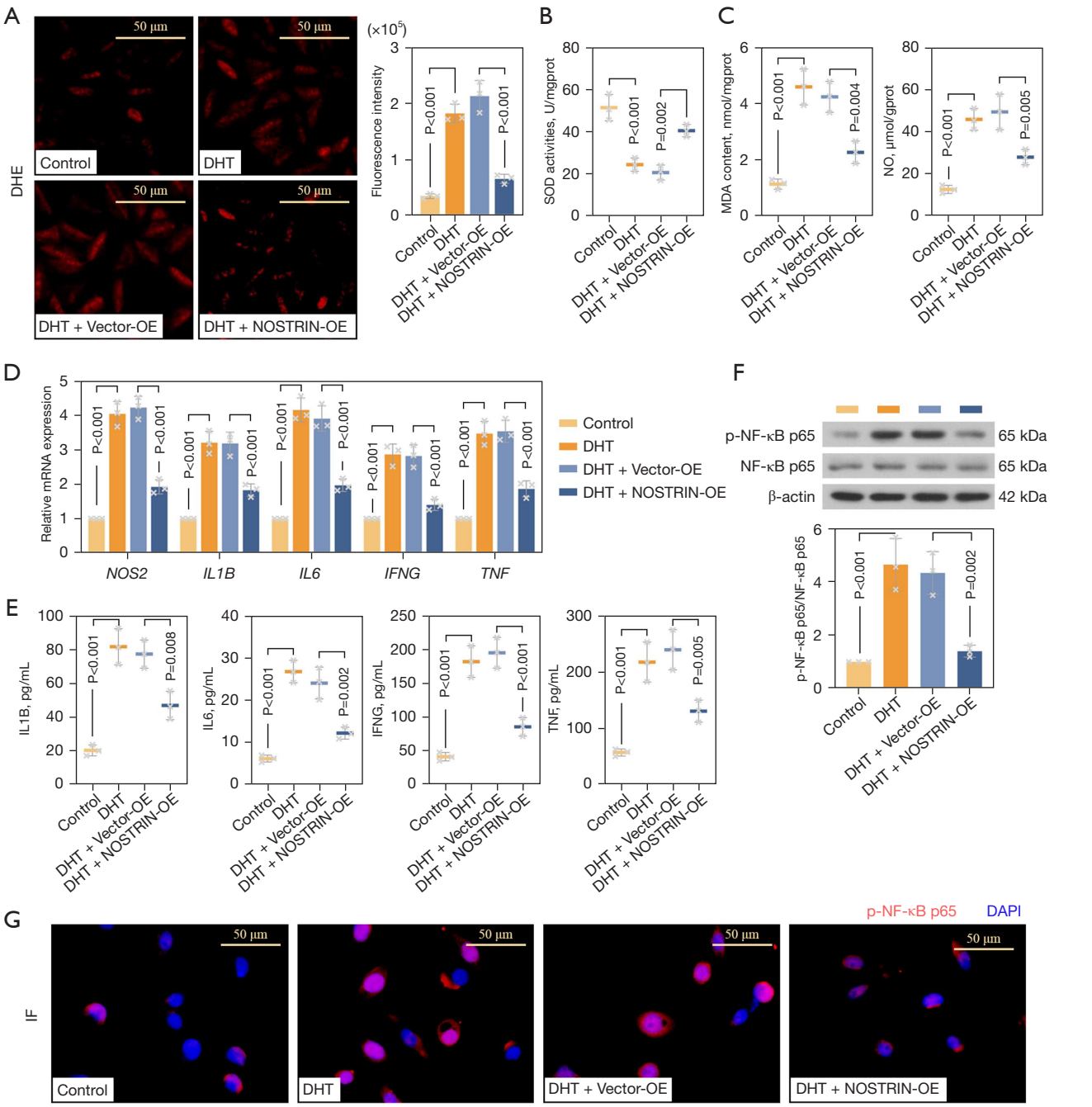

Figure 4 NOSTRIN overexpression reduces oxidative stress and inflammation and inhibits NF-κB signaling in dihydrotestosterone-induced RWPE-1 cells. (A) Representative images of DHE staining (400×) and quantification of fluorescence intensity. (B) SOD activities in the indicated groups. (C) MDA and NO contents in RWPE-1 cells. (D) Relative mRNA expression levels of nitric oxide synthase 2 (*NOS2*), interleukin 1 beta (*IL1B*), interleukin 6 (*IL6*), interferon gamma (*IFNG*), and tumor necrosis factor (*TNF*) in RWPE-1 cells. (E) The concentration of IL1B, IL6, IFNG, and TNF in the supernatant was measured by enzyme-linked immunosorbent assay. (F) Western blot analysis of NF-κB p65 and phospho-NF-κB p65. (G) Immunofluorescence images (400×) of phospho-NF-κB p65 (p-NF-κB p65). Data are shown as mean ± standard deviation. The P value and scale bar are marked in the figure. DHT, dihydrotestosterone; NOSTRIN, nitric oxide synthase traffic inducer; OE, overexpression; NF-κB, nuclear factor-kappa B; SOD, superoxide dismutase; MDA, malondialdehyde; NO, nitric oxide; DHE, dihydroethidium.

epithelial cells (25) and it is a reliable marker for BPH. The PSA protein expression was significantly increased in the hyperplastic prostate of mice. Remarkably, overexpression of NOSTRIN reduced the protein expression of PSA in epithelial cells, indicating that NOSTRIN exhibited an inhibitory effect on BPH. One of the characteristics of BPH is the non-malignant proliferation of epithelial cells (26). The overexpressed NOSTRIN notably inhibited the protein expression of PCNA, as well as reduced the epithelial cell proliferation *in vitro*. CDK4 and CCND1 are key effectors regulating cell cycle transition (23). NOSTRIN overexpression inhibited the proliferation of epithelial cells in part by suppressing these cell cycle-related proteins expression. These findings implied that overexpressed-NOSTRIN may have improvements against BPH by reducing the PSA expression and proliferation of prostate epithelial cells.

Oxidative stress is recognized as a major factor in the progression of BPH (4,27). Many previous reports have shown that agents with antioxidant properties exhibit a protective effect on the progression of BPH (18,28-30). In the present study, the overexpression of NOSTRIN markedly inhibited the production of ROS, MDA, and NO and increased the SOD activity *in vitro*, implying that NOSTRIN may ameliorate BPH through suppressing oxidative stress in prostate epithelial cells.

Prostatic inflammation is another important contributing factor in the pathogenesis of BPH (31,32). It has been reported that high-grade prostatic inflammation is positively correlated with the symptom score and prostate volume of patients with BPH (6). Furthermore, several researches have shown that protective agents have anti-inflammatory properties in testosterone-induced BPH (18,33,34). In the endothelial cells, overexpression of NOSTRIN was reported to down-regulate the mRNA expression of *Il6*, a cytokine regulating inflammation (15). Similarly, the mRNA and protein expression of IL6 was significantly inhibited in NOSTRIN-overexpressed epithelial cells. In addition, the crucial inflammatory mediators in the prostatic tissues, NOS2 (18), IL1B (35), TNF (36), and IFNG (37), were notably decreased in the NOSTRIN-overexpressing prostatic epithelial cells. These results indicated that NOSTRIN overexpression may protect against BPH through its anti-inflammatory effects in prostatic epithelial cells.

NF-κB is a key transcription factor that regulates cell proliferation, oxidative stress, and inflammation (20,38). We observed increasing phosphorylation levels of NF-κB p65 in the prostate tissues of mice with BPH, suggesting the activation of NF-κB signaling. This finding was similar to a previous study (39). Interestingly, NOSTRIN has been reported to directly interact with TNF receptor-associated factor 6 (TRAF6), and lead to the inhibition of NF-κB activity in endothelial cells (15). Furthermore, NOSTRIN can reverse the NF-κB pathway activation induced by TNF-α in endothelial cells (15). Similarly, in our *in vitro* experiment, the overexpression of NOSTRIN significantly declined the phosphorylation level of NF-κB p65. This finding suggested that NOSTRIN may inhibit cell proliferation, oxidative stress, and inflammation by suppressing the NF-κB signals in prostatic epithelial cells. Whether NOSTRIN exerts this effect through interacting with TRAF6 needs further exploration.

Besides T-cells, macrophages are the main inflammatory cell type infiltrating the prostate during BPH (40). Our results in the mouse BPH model support this finding. Generally, the macrophages could be divided into the pro-inflammatory M1 phenotype and the anti-inflammatory M2 phenotype. Jin and coworkers (39) found that the mRNA expression of M1 macrophage markers was significantly increased in prostate tissues of rats with BPH, whereas M2 macrophage markers were inhibited. We have demonstrated that prostate epithelial cells produce and release pro-inflammatory mediators including *TNF* and *IFNG* in response to the DHT stimulation. TNF and IFNG potently induce M1 macrophage activation (41). Overexpression of NOSTRIN might prevent the macrophage transition to pro-inflammatory M1 phenotype by inhibiting the production of these pro-inflammatory mediators in prostate epithelial cells. However, one limitation is that we investigated the anti-inflammatory effects of NOSTRIN only in RWPE-1 epithelial cells without correlation with macrophages. Further study is needed to explore the relationship between prostate epithelial cells and other involved cells as macrophages and the effect of NOSTRIN *in vivo*. In addition, this study has so far only explored the role of NOSTRIN overexpression on BPH. To fully elucidate its roles, studies may be needed by silencing NOSTRIN at cell or animal levels. Challenges remain in translating our promising initial findings into clinical practice.

Conclusions

In conclusion, our study demonstrated the protective role

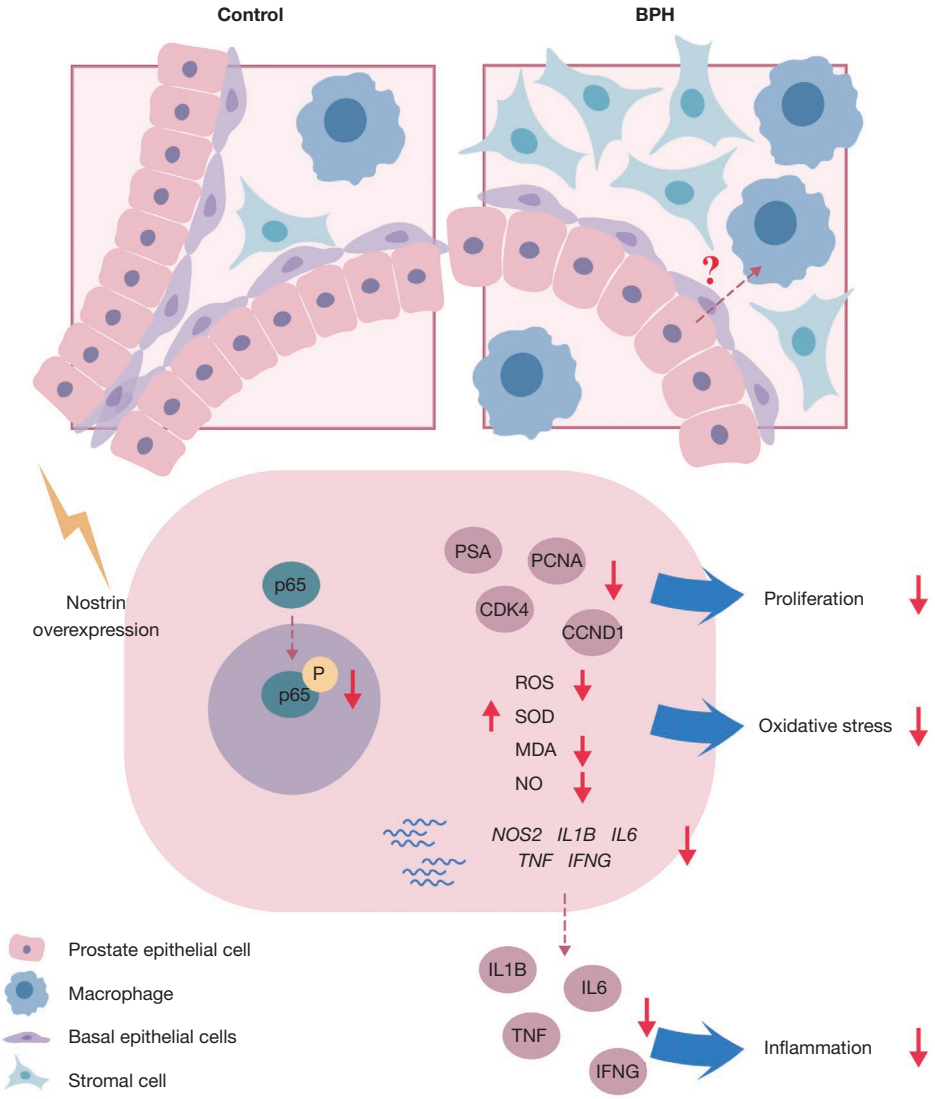

Figure 5 Graphical abstract. NOSTRIN overexpression alleviated the pathogenesis of BPH probably by inhibiting cell proliferation, oxidative stress, and inflammation through the inhibition of NF-κB signaling in prostate epithelial cells. NOSTRIN, nitric oxide synthase traffic inducer; BPH, benign prostatic hyperplasia; NF-κB, nuclear factor-kappa B; PSA, prostate-specific antigen; PCNA, proliferating cell nuclear antigen; CDK4, cyclin dependent kinase 4; CCND1, cyclin D1; ROS, reactive oxygen species; SOD, superoxide dismutase; MDA, malondialdehyde; NO, nitric oxide; NOS2, nitric oxide synthase 2; IL1B, interleukin 1 beta; IL6, interleukin 6; TNF, tumor necrosis factor; IFNG, interferon gamma.

of NOSTRIN in proliferating prostate epithelial cells. NOSTRIN expression was significantly reduced in both the prostate tissues of mice with BPH and DHT-induced RWPE-1 cells. NOSTRIN overexpression remarkedly inhibited RWPE-1 cell proliferation by suppressing CDK4 and CCND1 protein expression. In RWPE-1 cells treated with DHT, NOSTRIN overexpression notably suppressed oxidative stress and inflammation and inhibited NF-κB signaling. The schematic diagram of the proposed mechanism is shown in the Graphical abstract (*Figure 5*).

These results demonstrate an involvement of NOSTRIN in BPH identifying NOSTRIN as a potential therapeutic target for ameliorating BPH.

Acknowledgments

Funding: This research was supported by the Key Research and Development Program of Hebei Province (No. 22377796D to S.L.).

Footnote

Reporting Checklist: The authors have completed the ARRIVE reporting checklist. Available at https://tau.amegroups.com/article/view/10.21037/tau-24-209/rc

Data Sharing Statement: Available at https://tau.amegroups.com/article/view/10.21037/tau-24-209/dss

Peer Review File: Available at https://tau.amegroups.com/article/view/10.21037/tau-24-209/prf

Conflicts of Interest: All authors have completed the ICMJE uniform disclosure form (available at https://tau.amegroups.com/article/view/10.21037/tau-24-209/coif). S.L. reports the funding from the Key Research and Development Program of Hebei Province (No. 22377796D). The other authors have no conflicts of interest to declare.

Ethical Statement: The authors are accountable for all aspects of the work in ensuring that questions related to the accuracy or integrity of any part of the work are appropriately investigated and resolved. Experiments were performed under a project license (No. 202372) granted by the Ethics Committee of Hebei General Hospital, in compliance with institutional guidelines for the care and use of animals.

References

1. Sarma AV, Wei JT. Clinical practice. Benign prostatic hyperplasia and lower urinary tract symptoms. N Engl J Med 2012;367:248-57.
2. Chughtai B, Forde JC, Thomas DD, et al. Benign prostatic hyperplasia. Nat Rev Dis Primers 2016;2:16031.
3. Sharma M, Chadha R, Dhingra N. Phytotherapeutic Agents for Benign Prostatic Hyperplasia: An Overview. Mini Rev Med Chem 2017;17:1346-63.
4. Quintero-García M, Delgado-González E, Sánchez-Tusie A, et al. Iodine prevents the increase of testosterone-induced oxidative stress in a model of rat prostatic hyperplasia. Free Radic Biol Med 2018;115:298-308.
5. Kramer G, Mitteregger D, Marberger M. Is benign prostatic hyperplasia (BPH) an immune inflammatory disease? Eur Urol 2007;51:1202-16.
6. Robert G, Descazeaud A, Nicolaïew N, et al. Inflammation in benign prostatic hyperplasia: a 282 patients' immunohistochemical analysis. Prostate 2009;69:1774-80.
7. De Nunzio C, Presicce F, Tubaro A. Inflammatory mediators in the development and progression of benign prostatic hyperplasia. Nat Rev Urol 2016;13:613-26.
8. Vanli N, Sheng J, Li S, et al. Ribonuclease 4 is associated with aggressiveness and progression of prostate cancer. Commun Biol 2022;5:625.
9. Heidenreich A, Bellmunt J, Bolla M, et al. EAU guidelines on prostate cancer. Part 1: screening, diagnosis, and treatment of clinically localised disease. Eur Urol 2011;59:61-71.
10. Kovacevic I, Hu J, Siehoff-Icking A, et al. The F-BAR protein NOSTRIN participates in FGF signal transduction and vascular development. EMBO J 2012;31:3309-22.
11. Chakraborty S, Ain R. NOSTRIN: A novel modulator of trophoblast giant cell differentiation. Stem Cell Res 2018;31:135-46.
12. Wang J, Yang S, He P, et al. Endothelial Nitric Oxide Synthase Traffic Inducer (NOSTRIN) is a Negative Regulator of Disease Aggressiveness in Pancreatic Cancer. Clin Cancer Res 2016;22:5992-6001.
13. Kirsch T, Kaufeld J, Korstanje R, et al. Knockdown of the hypertension-associated gene NOSTRIN alters glomerular barrier function in zebrafish (Danio rerio). Hypertension 2013;62:726-30.
14. Kovacevic I, Müller M, Kojonazarov B, et al. The F-BAR Protein NOSTRIN Dictates the Localization of the Muscarinic M3 Receptor and Regulates Cardiovascular

Function. Circ Res 2015;117:460-9.
15. Chakraborty S, Ain R. Nitric-oxide synthase trafficking inducer is a pleiotropic regulator of endothelial cell function and signaling. J Biol Chem 2017;292:6600-20.
16. Paul M, Gope TK, Das P, et al. Nitric-Oxide Synthase trafficking inducer (NOSTRIN) is an emerging negative regulator of colon cancer progression. BMC Cancer 2022;22:594.
17. Adaramoye OA, Oladipo TD, Akanni OO, et al. Hexane fraction of Annona muricata (Sour sop) seed ameliorates testosterone-induced benign prostatic hyperplasia in rats. Biomed Pharmacother 2019;111:403-13.
18. Abdel-Aziz AM, Gamal El-Tahawy NF, Salah Abdel Haleem MA, et al. Amelioration of testosterone-induced benign prostatic hyperplasia using febuxostat in rats: The role of VEGF/TGFβ and iNOS/COX-2. Eur J Pharmacol 2020;889:173631.
19. Holditch SJ, Brown CN, Lombardi AM, et al. Recent Advances in Models, Mechanisms, Biomarkers, and Interventions in Cisplatin-Induced Acute Kidney Injury. Int J Mol Sci 2019;20:3011.
20. Baeuerle PA, Henkel T. Function and activation of NF-kappa B in the immune system. Annu Rev Immunol 1994;12:141-79.
21. Zou Y, Aboshora W, Li J, et al. Protective Effects of Lepidium meyenii (Maca) Aqueous Extract and Lycopene on Testosterone Propionate-Induced Prostatic Hyperplasia in Mice. Phytother Res 2017;31:1192-8.
22. Jin BR, An HJ. Baicalin alleviates benign prostate hyperplasia through androgen-dependent apoptosis. Aging (Albany NY) 2020;12:2142-55.
23. Yu XN, Zhang GC, Liu HN, et al. Pre-mRNA processing factor 19 functions in DNA damage repair and radioresistance by modulating cyclin D1 in hepatocellular carcinoma. Mol Ther Nucleic Acids 2021;27:390-403.
24. Zimmermann K, Opitz N, Dedio J, et al. NOSTRIN: a protein modulating nitric oxide release and subcellular distribution of endothelial nitric oxide synthase. Proc Natl Acad Sci U S A 2002;99:17167-72.
25. Lee KY, Kim SH, Yang WK, et al. Effect of Tetragonia tetragonoides (Pall.) Kuntze Extract on Andropause Symptoms. Nutrients 2022;14:4572.
26. Gong GY, Xi SY, Li CC, et al. Bushen Tongluo formula ameliorated testosterone propionate-induced benign prostatic hyperplasia in rats. Phytomedicine 2023;120:155048.
27. Choi YJ, Wedamulla NE, Kim SH, et al. Salvia miltiorrhiza Bunge Ameliorates Benign Prostatic Hyperplasia through Regulation of Oxidative Stress via Nrf-2/HO-1 Activation. J Microbiol Biotechnol 2024;34:1059-72.
28. Wu X, Gu Y, Li L. The anti-hyperplasia, anti-oxidative and anti-inflammatory properties of Qing Ye Dan and swertiamarin in testosterone-induced benign prostatic hyperplasia in rats. Toxicol Lett 2017;265:9-16.
29. Pawlicki B, Zielinski H, Dabrowski M. Role of apoptosis and chronic prostatitis in the pathogenesis of benign prostatic hyperplasia. Pol Merkur Lekarski 2004;17:307-10.
30. Ammar AE, Esmat A, Hassona MD, et al. The effect of pomegranate fruit extract on testosterone-induced BPH in rats. Prostate 2015;75:679-92.
31. Gandaglia G, Briganti A, Gontero P, et al. The role of chronic prostatic inflammation in the pathogenesis and progression of benign prostatic hyperplasia (BPH). BJU Int 2013;112:432-41.
32. Bello II, Omigbodun A, Morhason-Bello I. Common salt aggravated pathology of testosterone-induced benign prostatic hyperplasia in adult male Wistar rat. BMC Urol 2023;23:207.
33. Sayed RH, Saad MA, El-Sahar AE. Dapoxetine attenuates testosterone-induced prostatic hyperplasia in rats by the regulation of inflammatory and apoptotic proteins. Toxicol Appl Pharmacol 2016;311:52-60.
34. Atawia RT, Mosli HH, Tadros MG, et al. Modulatory effect of silymarin on inflammatory mediators in experimentally induced benign prostatic hyperplasia: emphasis on PTEN, HIF-1α, and NF-κB. Naunyn Schmiedebergs Arch Pharmacol. 2014;387:1131-40.
35. Choi DH, Kim JY, An JH, et al. Effects of Saussurea costus on apoptosis imbalance and inflammation in benign prostatic hyperplasia. J Ethnopharmacol 2021;279:114349.
36. Rho J, Seo CS, Park HS, et al. Asteris Radix et Rhizoma suppresses testosterone-induced benign prostatic hyperplasia in rats by regulating apoptosis and inflammation. J Ethnopharmacol 2020;255:112779.
37. Royuela M, de Miguel MP, Ruiz A, et al. Interferon-gamma and its functional receptors overexpression in benign prostatic hyperplasia and prostatic carcinoma: parallelism with c-myc and p53 expression. Eur Cytokine Netw 2000;11:119-27.
38. Barber K, Mendonca P, Evans JA, et al. Antioxidant and Anti-Inflammatory Mechanisms of Cardamonin through Nrf2 Activation and NF-kB Suppression in LPS-Activated BV-2 Microglial Cells. Int J Mol Sci 2023;24:10872.
39. Jin BR, An HJ. Oral administration of berberine represses macrophage activation-associated benign prostatic

hyperplasia: a pivotal involvement of the NF-κB. Aging (Albany NY) 2021;13:20016-28.
40. Tang J, Yang J. Etiopathogenesis of benign prostatic hypeprlasia. Indian J Urol 2009;25:312-7.
41. Mosser DM, Edwards JP. Exploring the full spectrum of macrophage activation. Nat Rev Immunol 2008;8:958-69.

Cite this article as: Li S, Yu C, Xiao H, Xu Q, Gao B, Guo L, Sun Z, Liu J. NOSTRIN is involved in benign prostatic hyperplasia via inhibition of proliferation, oxidative stress, and inflammation in prostate epithelial cells. Transl Androl Urol 2024;13(9):2055-2069. doi: 10.21037/tau-24-209